RESEARCH PAPER

PCCP
www.rsc.org/pccp

Barrier-free proton transfer in anionic complex of thymine with glycine

Iwona Dąbkowska,[ab] Janusz Rak,[a] Maciej Gutowski,*[c] J. Michael Nilles,[d] Sarah T. Stokes,[d] Dunja Radisic[d] and Kit H. Bowen Jr.[d]

[a] *Department of Chemistry, University of Gdańsk, Sobieskiego 18 80-952, Gdańsk, Poland*
[b] *Institute of Organic Chemistry and Biochemistry, Academy of Sciences of the Czech Republic, Flemingovo nam. 2 166 10, Prague 6, Czech Republic*
[c] *Chemical Sciences Division, Pacific Northwest National Laboratory, Richland WA 99352, USA*
[d] *Department of Chemistry, Johns Hopkins University, Baltimore MD 21218, USA*

Received 30th April 2004, Accepted 14th June 2004
First published as an Advance Article on the web 6th July 2004

We report the photoelectron spectrum of the thymine–glycine anionic complex (TG^-) recorded with low energy photons (2.540 eV). The spectrum reveals a broad feature with a maximum between 1.6–1.9 eV. The measured electron vertical detachment energy is too large to be attributed to a complex in which an anion of intact thymine is solvated by glycine, or vice versa. The experimental data are paralleled by electronic structure calculations carried out at the density functional theory level with 6-31++G** basis sets and the B3LYP and MPW1K exchange–correlation functionals. The critical structures are further examined at the second order Møller–Plesset level of theory. The results of calculations indicate that the excess electron attachment to the complex induces an intermolecular barrier-free proton transfer from the carboxylic group of glycine to the O8 atom of thymine. As a result, the four most stable structures of the thymine–glycine anionic complex can be characterized as a neutral radical of hydrogenated thymine solvated by an anion of deprotonated glycine. The calculated vertical electron detachment energies for the four most stable anionic complexes lie in a range 1.6–1.9 eV, in excellent agreement with the maximum of the photoelectron peak.

1. Introduction

There are two major issues which we address in this study: (i) interaction of low energy electrons with the gas-phase thymine–glycine complex, and (ii) intermolecular proton transfer in this complex induced by an excess electron.

Low-energy electrons appear as secondary products of radiolysis of water, with the primary products being the OH and H radicals.[1] Until now, the genotoxicity of radiation was primarily studied in the context of these radicals, and the connection between their presence and mutations of DNA is well documented.[2,3] The results of recent experiments by Sanche and coworkers suggest that electrons with energies in a range 1–20 eV can induce DNA damage.[4,5] The authors suggested that excess electrons trapped in temporary anionic states initiate chemical reactions leading to single- and double-strand breaks. A few estimations of the activation barrier needed to rupture the sugar-phosphate bond have been made.[6,7] However, the mechanism, leading from anionic states localized on nucleic acid bases to strand breaks, has been only briefly studied.

Electron trapping on nucleic acid bases has been an important topic in radiation biology for several decades.[8–15] About ten years ago, it was realized that the high polarity of these molecules allows for the existence of dipole-bound anionic states as well.[13] While our recent CCSD(T) results indicate that the valence anionic state of thymine (T) is vertically stable with respect to the neutral by 0.457 eV, our calculations also find the valence anionic state to be adiabatically unstable by 0.248 eV with respect to the dipole-bound anionic state and by 0.196 eV with respect to the neutral.[16] The results of low-energy electron transmission spectroscopy experiments suggest that the valence anionic state is also unbound at the geometry of the neutral.[17] The current view is that the valence anionic states of isolated nucleic acid bases are unbound, or at best, very weakly bound, although bound states dominate for solvated species.[14,15]

The intra- and intermolecular tautomerizations involving nucleic acid bases have long been suggested as critical steps in mutations of DNA.[14,18] Intramolecular proton transfer reactions have been studied for both isolated and hydrated nucleic acid bases.[8,19] Intermolecular single and double proton transfer reactions have been studied for the dimers of nucleic acid bases in both their ground and excited electronic states.[20,21] Only small activation barriers were found for both the anionic and cationic GC pair, with the proton transfer reaction being favorable for the anion and slightly unfavorable for the cation.[20]

Recently we described a proton transfer process, which is induced by the attachment of an excess electron to the complex of uracil (U) with proton donors, such as glycine,[22] alanine,[23] formic acid,[24] model inorganic acids,[25,26] and alcohols.[27] Denoting a proton donor as HA, the following process was identified:

$$U\cdots HA + e^- \rightarrow UH^{\bullet}\cdots A^- \qquad (1)$$

Our *ab initio* calculations and photoelectron spectroscopy measurements (PES) strongly suggested that the electron attachment to complexes of uracil with some of these HA's leads to a barrier-free proton transfer (BFPT) from the acid (HA) to the O8 atom of U, with the product dimer complex being a neutral radical of hydrogenated uracil ($UH^{\bullet}$) and A^-. The driving force for proton transfer is the stabilization of the excess electron onto the π^* orbital of the base. Thus, one may envision the process as one in which the excess electron first attaches itself to the nucleic acid base moiety of the dimer,

DOI: 10.1039/b406455k

forming an ultra-basic anion, which then extracts a proton from the proton donor portion of the dimer to yield the complex, $UH^{\bullet}\cdots A^{-}$.

Our previous studies were limited to complexes of uracil with various HA's and we discussed the occurrence of BFPT as an outcome of the interplay between the deprotonation energy of HA, protonation energy of U^{-}, and the energy of intermolecular hydrogen bonds.[22–27] Our results strongly suggested that alanine and phenylalanine act in a similar way as does glycine in its anionic dimeric complexes with uracil.[22,23] Thus, the BFPT process was not very sensitive to the nature of the amino acid's hydrophobic residual group.

Another intriguing question is whether other nucleic acid bases are also susceptible to BFPT. We have recently found that BFPT also occurs in anionic complexes of thymine (T) with formic acid (F) though a difference in the photoelectron spectra of UF^{-} and TF^{-} suggested that the methyl group of thymine could make a difference in the intermolecular proton transfer to the O8 atom (see Fig. 1 for the numbering of atoms in T).[24]

In the present study we further explore the effect of methylation of the C5 atom of uracil. We investigate anionic complexes of thymine–glycine (TG^{-}) and we compare the results with those for the UG^{-} complex.[22] The photoelectron spectra of UG^{-} and TG^{-} as well as the results of *ab initio* calculations strongly suggest that both nucleic acid bases undergo BFPT in anionic complexes with glycine. Moreover, a difference between U and T in the susceptibility to BFPT is much smaller in complexes with glycine than with formic acid.

An interesting point here is that attachment of low-energy electrons to complexes of RNA or DNA with proteins may also lead to mutations. While UG^{-} and TG^{-} dimer complexes are only primitive models of such processes, our results demonstrate the possibility of electron-induced mutations in DNA-peptide complexes. The formation of neutral radicals of hydrogenated pyrimidine nucleic acid bases could also play a role in damage to DNA and RNA by low energy electrons. For instance, thymine hydrogenated at the O8 position cannot form a hydrogen bond with adenine, as dictated by the Watson–Crick pairing scheme. We have also found that the radical, $TH^{\bullet}$ has a significant electron affinity.[16] Thus, the resulting anion, TH^{-}, might react with an adjacent deoxyribose molecule triggering strand-breaks in nucleic acids.[28]

2. Methods

2.1. Experimental

Negative ion photoelectron spectroscopy is conducted by crossing a mass-selected beam of negative ions with a fixed-frequency laser beam and energy-analyzing the resultant photodetached electrons.[29] It is governed by the energy-conserving relationship: $h\nu = \mathrm{EBE} + \mathrm{EKE}$, where $h\nu$ is the photon energy, EBE is the electron binding energy, and EKE is the electron kinetic energy. One knows the photon energy of the experiment, one measures the electron kinetic energy spectrum, and then by difference, one obtains electron binding energies, which in effect are the transition energies from the anion to the various energetically-accessible states of its corresponding neutral.

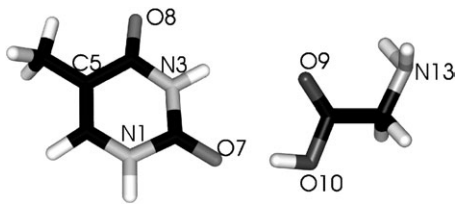

Fig. 1 The lowest energy tautomer of thymine and lowest energy conformer of glycine.

Our apparatus has been described elsewhere.[30] To prepare the species of interest, a mixture of thymine and glycine was placed in the stagnation chamber of a nozzle source and heated to ~180 °C. Argon gas at a pressure of 1–2 atm was used as the expansion gas. The nozzle diameter was 25 μm. Electrons were injected into the emerging jet expansion from a biased Th/Ir filament in the presence of an axial magnetic field. The resulting anions were extracted and mass-selected with a magnetic sector mass spectrometer. Electrons were then photodetached from the selected anions with ~100 circulating Watts of 2.540 eV photons and then energy-analyzed with a hemispherical electron energy analyzer. The temperature of mass-selected anions is not known, but based on the source conditions utilized, it likely lies between 100 K and 300 K.

2.2. Computational

As this computational effort is a continuation of our previous studies on the neutral[31] and anionic[22] complexes of uracil and glycine, we will use analogous notation for hydrogen-bonded structures and the same computational methodology. The anionic structures characterized in the current study will be labeled as aTGn, indicating the *parent* neutral structure TGn the anionic structure is related to. More precisely, an anionic structure aTG*n* is determined in the course of geometry optimization initialized from the optimal geometry for the neutral structure TG*n*. The structures TG*n* for the neutral thymine–glycine complexes are analogous to the uracil–glycine UG*n* structures characterized in ref. 31.

The stability of the neutral (superscript = 0) or anionic (superscript = −) TG complexes is expressed in terms of E_{stab}, H_{stab}, and G_{stab}. E_{stab} is defined as a difference in electronic energies of the monomers and the dimer:

$$E_{\mathrm{stab}} = E^{\mathrm{TG}^{(0,-)}}(G^{\mathrm{TG}^{(0,-)}}) - E^{\mathrm{TG}^{(0,-)}}(G^{\mathrm{T}^{(0,-)}}) - E^{\mathrm{G}}(G^{\mathrm{G}}) \quad (2)$$

with the electronic energy E^{X} ($\mathrm{X} = \mathrm{T}^{(0,-)}$, G, $\mathrm{TG}^{(0,-)}$) computed for the coordinates determining the optimal geometry of X (*i.e.*, the geometry where E^{X} is at the minimum). The values of E_{stab} were not corrected for basis set superposition errors because our earlier results demonstrated that the values of this error in B3LYP/6-31++G** calculations for a similar neutral uracil–glycine complex did not exceed 0.06 eV.[31] The stabilization enthalpy H_{stab} results from correcting E_{stab} for zero-point vibration terms, thermal contributions to energy from vibrations, rotations, and translations, and the pV terms. Finally, the stabilization Gibbs energy G_{stab} results from supplementing H_{stab} with the entropy term. The values of H_{stab} and G_{stab} discussed below were obtained for $T = 298$ K and $p = 1$ atm in the harmonic oscillator-rigid rotor approximation. The selection of $T = 298$ K was not dictated by the temperature of mass selected anions, because the latter is not known precisely. It was chosen instead as a temperature which is reasonable for biological systems.

As our primary research method we applied density functional theory (DFT)[32,33] with a Becke's three parameter hybrid functional (B3LYP)[34–36] and a modified Perdew-Wang 1-parameter-method for kinetics (MPW1K) designed by Truhlar *et al.*[37] In both DFT approaches we used the same 6-31++G** basis set.[38] Five d functions were used on heavy atoms. The usefulness of the B3LYP/6-31++G** method to describe intra- and intermolecular hydrogen bonds has been demonstrated in recent studies through comparison with the second order Møller–Plesset (MP2) predictions.[31,39] The ability of the B3LYP method to predict excess electron binding energies has recently been reviewed and the results were found to be satisfactory for valence-type molecular anions.[40] We found that the value of electron vertical detachment energy (VDE) determined at the B3LYP/6-31++G** level for the valence π* anionic state of an isolated thymine is overestimated by 0.2 eV in comparison with the CCSD(T)/aug-cc-pVDZ

result. We will assume in the following that the same correction of 0.2 eV applies to the values of the VDE for all anionic TG complexes in which an excess electron occupies a π* orbital localized on thymine.

It is known that the B3LYP method underestimates barriers for proton transfer reactions,[37] and thus lack of a barrier for the proton transfer reaction may be an artifact of the B3LYP method. For this reason, we performed additional geometry optimizations using the MPW1K exchange–correlation functional, which was parameterized to reproduce barrier heights for chemical reactions.[37] Finally, MP2 geometry optimizations have been performed for three anionic TG complexes to demonstrate consistency among different theoretical models and therefore to strengthen our conclusion. The same 6-31++G** basis set was used in the B3LYP, MPW1K and MP2 calculations.

The presence of many low energy structures for neutral and anionic complexes prompted us to determine the populations of these structures in the gas phase equilibrium. First, we selected a reference structure R for a given species (neutral or anionic). Next, for every structure M other than the reference structure R we determined the equilibrium constant K_M.

$$K_M = [M]/[R] \quad (3)$$

from the difference in Gibbs free energies for M and R. The fraction of M in the equilibrated sample is given by

$$x_M = K_M/(1 + K_1 + K_2 + \ldots) \quad (4)$$

where the sum in the denominator goes through all structures for a given species. The fraction of R in the sample is

$$x_R = 1/(1 + K_1 + K_2 + \ldots). \quad (5)$$

All calculations were carried out with the GAUSSIAN 98[38] and NWChem[41] codes on a cluster of 32 bit Xeon/SCI Dolphin processors, IBM SP/2, and SGI 2800, and Origin2000 numerical servers.

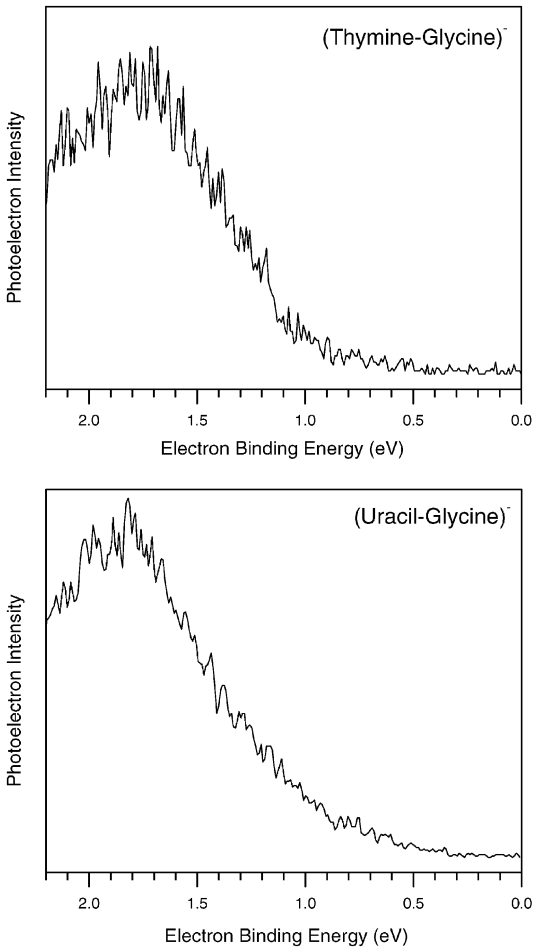

Fig. 2 Photoelectron spectrum of the dimer anion of thymine–glycine. For comparison, the spectra of dimer anion of uracil–glycine is also presented.[22] Both spectra recorded with 2.540 eV photon^{-1}.

3. Results

3.1. PES spectra

The photoelectron spectra for TG^- and UG^- are quite similar, see Fig. 2. Each spectrum exhibits a broad, structure-less feature. For TG^-, its maximum occurs at EBE = 1.6–1.9 eV, while for UG^-, its maximum occurs at EBE = 1.7–2.0 eV. The photoelectron spectrum of TG^- cannot be attributed to an intact T^- solvated by glycine. As mentioned above, the valence π* and dipole-bound anionic states of thymine are characterized by a calculated value of the VDE of 0.457 and 0.055 eV, respectively (see Fig. 3 for the excess electron charge distributions in these systems). Henceforth, only the valence π* anionic state will be considered further, since the experimental value of the VDE for TG^- is far too large for the dipole-bound anionic state of T solvated by G. However, the experimental value of the VDE is also too large for the valence π* anionic state of T solvated by G. The solvation energy by glycine would have to be larger by ~1.4 eV, for the anion over its corresponding neutral, in order to be consistent with the maximum in the photoelectron spectrum. This is rather improbable given that the VDE of $U^-(H2O)_1$ is only 0.9 eV.[9]

Similarly, attributing the broad peak for TG^- to an anion of intact glycine solvated by thymine is inappropriate. The reason is that the most stable conformer of canonical glycine (Fig. 1) does not bind an electron[42] and the measured EA of glycine is *ca.* −1.8 eV.[43] Our theoretical results indicate that glycine forms only weakly bound anions with the VDE values, determined at the CCSD(T) level, of 0.08 and 0.39 eV for the canonical (can) and zwitterionic (zwit) structure, respectively[42] (see Fig. 3 for the excess electron charge distributions in these

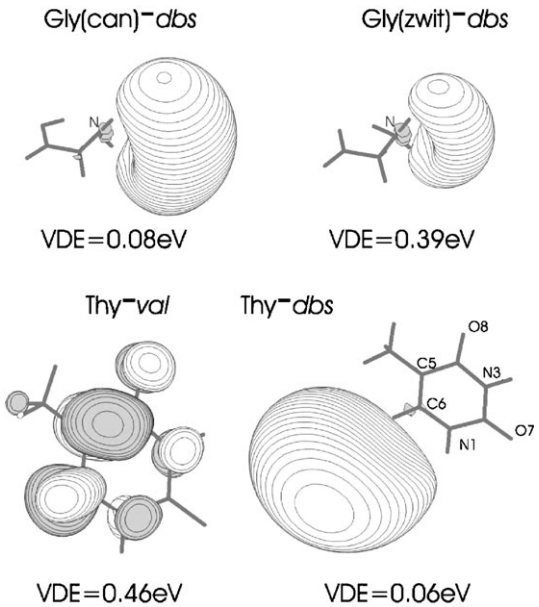

Fig. 3 The excess electron orbital for the valence π* and dipole-bound states of thymine (bottom) and dipole-bound anionic states of canonical and zwitterionic glycine (top). We have applied a contour line spacing of 0.03 $a_0^{-3/2}$ for the valence anion of thymine, 0.021 $a_0^{-3/2}$ for the dipole-bound state of zwitterionic glycine, and 0.008 $a_0^{-3/2}$ for the dipole-bound states of thymine and canonical glycine.

systems). The electron binding energy shift induced by the interaction with thymine would have to be again approximately 1.4 eV to be consistent with the maximum of the photoelectron peak for TG^-, which is rather improbable.

Thymine in anionic complexes with glycine behaves very much like uracil in anionic complexes with glycine (see Fig. 2). We expect that BFPT occurs in anionic complexes of glycine with thymine, in full analogy to the anionic uracil–glycine complexes.[22] However, there is also a difference in the photoelectron spectrum of TG^- relative to that of UG^-. When compared to the spectrum of UG^-, the photoelectron spectrum of TG^- appears to be shifted by about 0.1 eV towards smaller values of electron binding energy. This can be partially attributed to the difference in the VDE for isolated anions of thymine and uracil, 0.46 and 0.51 eV, respectively.[16] Interestingly, the difference between T and U is much more profound in anionic complexes with formic acid.[24]

Lastly, the widths of the main spectral features for TG^- and UG^- are much greater than of the photoelectron features for the valence anionic state of uracil solvated by either a single water molecule or a xenon atom.[9] While this is mainly additional evidence that these complexes are not valence anions of T or U solvated by glycine, it may also indicate that several conformers of the anionic T(U)-glycine complexes coexist in the gas phase under our experimental conditions.

3.2. Computational results

3.2.1. Neutral thymine–glycine complexes. Thymine and uracil differ only by a methyl group at the C5 position, with the proton acceptor C═O and proton donor N–H sites being the same. When compared to uracil, the methyl group in thymine can create at most steric obstacles that have to be negotiated upon formation of hydrogen bonds. In addition, a weak hydrogen bond with C5H acting as a weak proton donor, is operational only in complexes with uracil. The topological space for the neutral TG complex is at least as complicated as for the neutral UG complex. For the latter, we characterized twenty-three hydrogen-bonded structures formed by the lowest energy tautomers of U and G.[31] In the current study only a limited subset of these twenty-three structures was explored. We included the most stable structure of the neutral, which was labeled UG1 in ref. 31, plus all structures with the O8 atom involved in hydrogen bonding (labeled UG*n*, $n = 2$, 4, 14, 16, 18, and 20 in ref. 31), as we know from our earlier studies[22–27] that these latter complexes become the most stable upon an excess electron attachment.

The neutral TGn complexes are displayed in Fig. 4 and their B3LYP/6-31++G** characteristics are given in Table 1. The stability order follows the *n* index, which indicates that the stability order is the same for the UG and TG complexes, even though a weak hydrogen bond, with C5H acting as a weak proton donor, is not operational in the TG complexes. The most stable complexes are TG1 and TG2 with the carbonyl (O9) and hydroxyl (O10H) groups of glycine interacting with the proton donor and acceptor centers of thymine. The TG1 and TG2 structures have two strong hydrogen bonds and the values of E_{stab} are −0.72 and −0.61 eV, respectively. These stabilization energies are typical for dimers forming ring-like structures.[31] The values of G_{stab} are negative for these structures indicating a thermodynamic preference to form the thymine–glycine dimer. TG1 and TG2 are not connected by a simple reaction path as there is another ring-like structure, TG3, which separates them. The glycine moiety in TG3 is oppositely oriented than in TG1 and TG2. Thus, one can assume that a barrier along the path from TG1 to TG2 is approximately equal to the value of E_{stab} for TG1, which is significant for a room temperature transformation. The TG1 structure is important for gas phase studies of thymine as its percent share in equilibrium mixture at $T = 298.15$ K is 98%

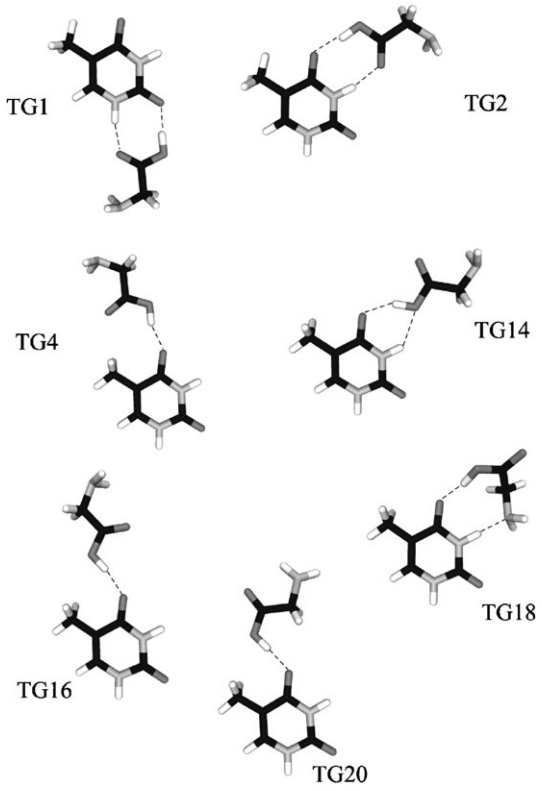

Fig. 4 Optimized structures of neutral complexes of glycine with thymine.

(see Table 1). In DNA, however, the N1 atom is covalently bonded to the sugar-phosphate backbone and the N1 site is not available for hydrogen bonding.

The TG4 structure, with one O8···H–O10 hydrogen bond, and the carbonyl O9 atom interacting with the methyl group is stable by only −0.38 eV in terms of E_{stab} and unstable in terms of G_{stab}, as are other TGn structures ($n = 14$, 16, 18, 20). The diminished stability of TG14 results from the fact that the O10H hydroxyl group acts as a proton donor *and* acceptor. The small stability of TG18 and TG20 results from a geometrical mismatch between the proton donor and acceptor sites of interacting monomers.[31] Additionally, the presence of the CH_3 group creates a steric obstacle that needs to be negotiated in the TG*n* ($n = 4$, 16, 20) structures. In fact, we observed substantial geometrical reorganizations with respect to the corresponding UG structures upon geometry optimization.

The dipole moments of thymine, glycine, and the neutral TG*n* complexes provide insight into whether anionic dipole-bound states can contribute to the photoelectron spectrum of $(TG)^-$ reported in Fig. 2. For the most stable conformer of canonical glycine, the B3LYP/6-31++G** dipole moment of 1.23 D is smaller than the critical dipole moment of *ca.* 2.5 D required for excess electron binding,[8] but a less stable canonical conformer is characterized by a larger dipole moment of 6.1 D. The calculated dipole moment of thymine is 4.7 D and the calculated dipole moments of the TG*n* complexes do not exceed 8.2 D. These dipole moments are too small to support a dipole-bound anionic state with a VDE of *ca.* 1.7 eV.[44] However, the dipole-bound anionic states supported by TG2-TG20 might act as doorways to valence anionic states characterized in Section 3.2.2. Finally, the electron binding energy at the maximum of the PES peak for TG^- is larger by one order of magnitude than the calculated value of the VDE for an excess electron solvated by glycine and uracil.[45] Thus a structure with an excess electron solvated by thymine and glycine is not considered in this study.

Table 1 Thymine–glycine neutral complexes' B3LYP/6-31++G** characteristics. Energies in eV, dipole moments, μ, in D. E_{stab} and G_{stab} stand for the energy and Gibbs free energy of stabilization, respectively (see eqn. (2)). ZPVE is a correction from zero-point vibrations. The percent share of each form in equilibrium mixture at $T = 298.15$ K is denoted by x (see eqns. (4) and (5))

Structure	E_{stab}	E_{stab} + ZPVE	G_{stab}	μ	x
TG1	−0.72	−0.67	−0.18	2.95	97.98
TG2	−0.61	−0.56	−0.08	6.04	2.02
TG4	−0.38	−0.33	0.10	4.86	0.00
TG14	−0.34	−0.30	0.11	7.15	0.00
TG16	−0.30	−0.27	0.11	7.10	0.00
TG18	−0.33	−0.26	0.23	8.22	0.00
TG20	−0.12	−0.08	0.32	7.44	0.00

3.2.2. Anionic thymine–glycine complexes. The results of B3LYP/6-31++G** calculations for anions of various hydrogen-bonded thymine–glycine complexes are summarized in Table 2, and representative structures are displayed in Fig. 5. A common feature of anionic wavefunctions identified by us for the TG complexes is that the excess electron is localized on a π^* orbital of thymine, in close resemblance to the valence anionic state of isolated thymine (see Figs. 3 and 5). Occupation of the antibonding π orbital by an excess electron induces buckling of the ring of thymine because non-planar structures are characterized by a less severe antibonding interaction.[11,22] The same kind of ring distortion takes place in all TG complexes upon excess electron attachment.

Our most important finding is that the most stable anionic TG structures are characterized by a BFPT from the carboxylic group of glycine to the O8 atom of thymine, see Table 2 and Fig. 5. This behavior is analogous to that reported for the UG^- complexes[22] and demonstrates that not only uracil but also thymine is susceptible to barrier-free intermolecular proton transfer. This also explains why the PES spectra of UG^- and TG^- are so similar (see Fig. 2).

The driving force for proton transfer in the TG^- complexes is to stabilize the excess negative charge, which is primarily localized in the O8–C4–C5–C6 region. In consequence of the extra stabilization of the excess electron provided by the transferred proton, the values of the VDE for the aTG2, aTG14, aTG4, aTG16 structures are larger by approximately 1.4 eV than for the valence anion of isolated thymine. In fact, the calculated values of the VDE for these structures span a range of 2.1–1.8 eV. After correcting downward by 0.2 eV, the resulting range of 1.9–1.6 eV coincides well with the broad peak in the photoelectron spectrum (see Fig. 2).

The products of the intermolecular proton transfer are the neutral radical TH, with the O8 atom hydrogenated, and the deprotonated glycine (see Fig. 5). We found that deprotonation of glycine requires, in terms of electronic energy, 15.1 eV. On the other hand, protonation of the valence anion of thymine provides, in terms of electronic energy, 14.7 eV. Hence, the occurrence of a hypothetical reaction, which leads to noninteracting products,

$$T^- + HOOC–CH_2–NH_2 \rightarrow TH^\bullet + {}^-OOC–CH_2–NH_2 \quad (6)$$

requires 0.4 eV. For the proton transfer to occur, the stabilizing interaction in the $TH^\bullet\cdots{}^-OOC–CH_2–NH_2$ system needs to: (i) compensate this barrier, and (ii) provide at least as much of the stabilization between the $TH^\bullet$ and $^-OOC–CH_2–NH_2$ systems as the untransformed T^- and $HOOC–CH_2–NH_2$ moieties could provide. Indeed, for the structures with BFPT, *i.e.*, aTG*n* (n = 2, 4, 14, 16), E_{stab} varies from −1.19 eV to −0.94 eV, whereas for the structures without BFPT, *i.e.*, aTG*n* (n = 1, 18, 20), the values of E_{stab} are smaller: -0.94 eV $< E_{stab} < -0.86$ eV. This confirms that occurrence of BFPT requires significant values of E_{stab} and that these would compensate the endothermicity of reaction (6).

The most stable structure of the anionic complex results from an excess electron attaching to TG2 and its population amounts to 87% at standard conditions. The neutral complex TG2 is less stable than TG1 by 0.1 eV, hence its population is only 2% at standard conditions (see Table 1). Upon electron attachment to TG2, the carboxylic proton is transferred without a barrier to the O8 atom and the B3LYP value of the VDE for the optimal anionic structure is 1.83 eV (see Table 2 and Fig. 5). The value of the VDE decreases to *ca.* 1.6 eV after correcting downward by 0.2 eV. For comparison, the calculated value of the VDE for the aTG1 complex, which does not undergo intermolecular proton transfer, is only 1.00 eV (0.8 eV after the 0.2 correction). For both structures the calculated values of adiabatic electron affinity are smaller by 0.6–1.2 eV than the VDE values.

The neutral structures TG4, TG14, and TG16, which in terms of E_{stab} are less stable than TG1 by 0.4, 0.3, and 0.3 eV, respectively, are strongly stabilized upon an excess electron attachment as they undergo a significant geometrical relaxation that includes barrier-free proton transfer. The resulting aTG14, aTG4, and aTG16 structures are more stable than the aTG1 structure and their B3LYP values of the VDE are

Table 2 Thymine–glycine anionic complexes' B3LYP/6-31++G** characteristics. Energies in eV. E_{stab} and G_{stab} stand for the energy and Gibbs free energy of stabilization, respectively, (see eqn. (2)). ZPVE is a correction from zero-point vibrations, VDE is the electron vertical detachment energy, and EA is adiabatic electron affinity. The percent share of each form in equilibrium mixture at $T = 298.15$ K is denoted by x (see eqns. (4) and (5)). Qualitative information (Yes/No) is provided as to whether an anionic structure undergoes BFPT with the B3LYP and MPW1K exchange–correlation functionals, as well as with the MP2 method (selected structures only)

Structure	E_{stab}	E_{stab} + ZPVE	G_{stab}	VDE	EA	x	BFPT B3LYP	BFPT MPW1K	BFPT MP2
aTG1	−0.94	−0.94	−0.48	1.00	0.44	0.02	No	No	No
aTG2	−1.19	−1.17	−0.69	1.83	0.68	87.38	Yes	Yes	Yes
aTG4	−0.97	−0.99	−0.53	1.95	0.48	0.19	Yes	Yes	Yes
aTG14	−1.08	−1.07	−0.64	2.07	0.56	11.66	Yes	Yes	
aTG16	−0.94	−0.98	−0.56	2.03	0.47	0.57	Yes	Yes	
aTG18	−0.86	−0.84	−0.33	1.37	0.33	0.00	No	No	
aTG20	−0.93	−0.96	−0.53	1.62	0.46	0.19	No	No	

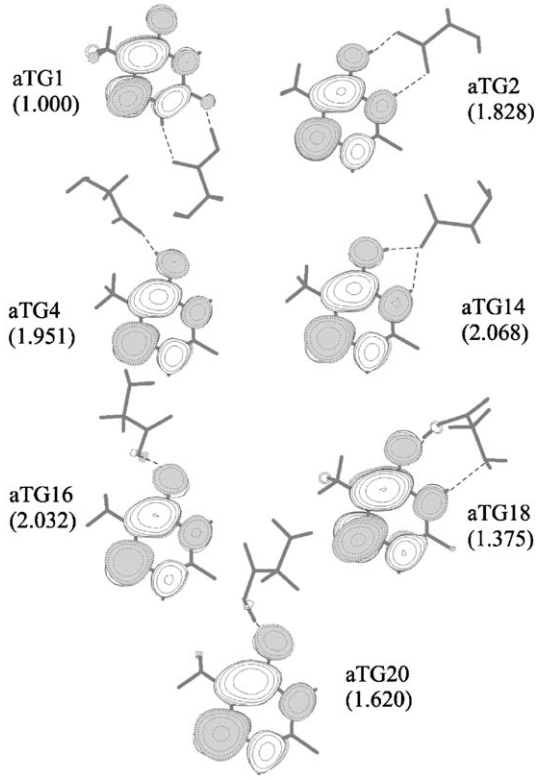

Fig. 5 The structure and excess electron charge distribution in the anionic thymine–glycine complexes. The orbitals were plotted with a contour line spacing of 0.03 $a_0^{-3/2}$. The B3LYP/6-31++G** values of electron vertical detachment energies are given in parentheses (eV).

2.1 (1.9), 2.0 (1.8) and 2.0 (1.8) eV, respectively (see Table 2 and Fig. 5; the corrected values are given in parentheses). These structures are less stable than aTG2 by only 0.2 eV. Their adiabatic electron affinities, calculated with respect to the parent neutral structures, were found to be 0.5–0.7 eV.

What topologically discriminates TG1 from other structures considered here is the fact that the O7 rather than O8 atom is involved in hydrogen bonding with glycine. The lack of BFPT for aTG1 may be related to the fact that an excess electron on the π^* orbital is not localized in the neighborhood of the O7 atom. This finding is important for gas phase studies of thymine, though in DNA the aTG1 structure is not operational because the N1 atom is covalently bonded to the sugar-phosphate backbone. aTG1 and aTG2 are not connected by a simple reaction path as there is another ring-like structure, aTG3, which separates them. The glycine moiety in aTG3 is oppositely oriented than in aTG1 and aTG2. Thus, one can assume that a barrier along the path from aTG1 to aTG2 is approximately equal to the value of E_{stab} for aTG1, which is significant for a room temperature transformation.

Finally, we should point out that not every hydrogen bond O10H$\cdots$O8 undergoes a BFPT upon attachment of an excess electron. The two structures TG18 and TG20 undergo just a serious structural reorganization upon an excess electron attachment, but not BFPT. The VDE values for aTG18 and aTG20 of 1.2 and 1.4 eV, respectively (after correcting downward by 0.2 eV), are remarkable for structures without a proton transferred to the ring of thymine and indicate an extra stabilization of the excess electron in T^- by 0.8–1.0 eV upon solvation by canonical glycine. A smaller value of the VDE for the aTG1 structure of 0.8 eV illustrates that the solvation at the O8 site provides more stabilization to the excess electron than solvation at the O7 site. Moreover, there is no local minimum on the potential energy surface of either aTG1, aTG18, or aTG20 with the O10H proton transferred to an oxygen atom of thymine.

The occurrence of BFPT (Yes/No in Table 2) proved to be consistent for the B3LYP and MPW1K methods. As a final verification, MP2/6-31++G** geometry optimizations were performed for the aTGn (n = 1, 2, 4) complexes starting from the geometry of the corresponding neutral complex. Again, BFPT occurred for $n = 2$ and 4 but not for $n = 1$. We conclude that the occurrence of BFPT is consistently predicted within various theoretical models, which strengthens our findings and interpretations.

There are at least four anionic structures aTGn (n = 4, 14, 16, 20), which differ in terms of G_{stab} by less than 0.16 eV from the most stable structure aTG2. The four structures susceptible to BFPT (n = 2, 4, 14, and 16) are characterized by large values of the VDE in a 1.6–1.9 eV range (after correcting downward by 0.2 eV). Of particular importance might be the aTG2 and aTG14 structure as their populations amount at standard conditions to 87 and 12%, respectively, and their values of the VDE differ by 0.2 eV. All these structures might contribute to the unusual width of the main feature in the photoelectron spectrum presented in Fig. 2.

Finally we comment on the differences in photoelectron spectra for TG^- and UG^-, see Fig. 2. A difference by about 0.1 eV in the maximum of the main feature is also confirmed by the B3LYP/6-31++G** results (Table 2 for TG^- and Table 1 in ref. 22 for UG^-). The calculated values of the VDE for the most stable anionic structure are 1.83 and 1.93 eV for TG^- and UG^-, respectively. The width of the main spectral feature might be slightly larger for TG^- than for UG^- and might be affected by the distribution of different structures and their values of the VDE. In addition there might be a contribution to the width of the PES feature of TG^- from the methyl group on thymine, which undergoes hindered rotations.

4. Summary

Our main findings are:

1. The photoelectron spectrum of the thymine–glycine anionic complex, recorded with 2.540 eV photons, reveals a broad feature with its maximum between EBE = 1.6–1.9 eV. The vertical electron detachment energy values are too large to be attributed to the complex of an anion of intact thymine solvated by glycine, or an anion of intact glycine solvated by thymine.

2. The theoretical results, obtained at the density functional theory and second order Møller–Plesset levels, indicate that excess electron can induce a barrier-free proton transfer from the carboxylic group of glycine to the O8 atom of thymine. The driving force for the proton transfer is to stabilize the negative excess charge localized primarily on the O8–C4–C5–C6 fragment of thymine.

3. The anionic complexes with the O8 site protonated are the most stable. These complexes can be viewed as the neutral radical of hydrogenated thymine solvated by the anion of deprotonated glycine and are characterized by the largest values of the VDE, which span a range of 1.9–1.6 eV. These values of the VDE were obtained by shifting the B3LYP values down by 0.2 eV, as suggested by the CCSD(T) results for the valence anionic state of isolated thymine.

4. The calculated values of the VDE for the most stable structures of TG^- are falling within the range observed in the PES spectrum. The measured PES spectra and theoretical results are similar for the UG^- and TG^- species suggesting that thymine behaves very much like uracil in anionic complexes with glycine. When compared to the spectrum of UG^-, the photoelectron spectrum of TG^- appears to be shifted by about 0.1 eV towards smaller values of electron binding energy. This can be partially attributed to the difference in the VDE for isolated anions of thymine and uracil, 0.46 and 0.51 eV, respectively.

5. The difference between T and U in anionic complexes with glycine is much less profound than in anionic complexes with formic acid. To elucidate these differences we are currently exploring anionic complexes with acid molecules bound to the C5 and C6 atoms of uracil or thymine.

6. The formation of neutral radicals of hydrogenated pyrimidine nucleic acid bases upon interaction with low energy electrons may be relevant to the damage of DNA and RNA. The mechanism of strand breaks triggered by these radicals is currently being investigated in our group.

Acknowledgements

This work was supported by the: (i) US DOE Office of Biological and Environmental Research, Low Dose Radiation Research Program (M.G.), (ii) NSF grant CHE-0211522 (K.B.), and (iii) Polish State Committee for Scientific Research (KBN) Grant 4 T09A 012 24. I.D. acknowledges International Visegrad Fund for financial support. The calculations were performed in the following computational centers: TASK in Gdansk, ICM in Warsaw (project nr G25-1), Cyfronet in Krakow (grant KBN/SGI2800/UGdanski/051/2002) and at the National Energy Research Scientific Computing Center (NERSC). PNNL is operated by Battelle for the U.S. DOE under Contract DE-AC06-76RLO 1830.

References

1 S. Steenken, *Chem Rev*., 1989, **89**, 503.
2 C. J. Burrows and J. G. Muller, *Chem. Rev*., 1998, **98**, 1109.
3 B. Armitage, *Chem. Rev*., 1998, **98**, 1171.
4 B. Boudaïffa, P. Cloutier, D. Hunting, M. A. Huels and L. Sanche, *Science*, 2000, **287**, 1658.
5 L. Sanche, *Mass Spectrom. Rev*., 2002, **21**, 349.
6 R. Barrios, P. Skurski and J. Simons, *J. Phys. Chem. A*, 2002, **106**, 7991.
7 X. Li, M. D. Sevilla and L. Sanche, *J. Am. Chem. Soc*., 2003, **125**(45), 13668.
8 C. Desfrancois, S. Carles and J. P. Schermann, *Chem. Rev*., 2000, **100**, 3943.
9 J. H. Hendricks, S. A. Lyapustina, H. L. deClercq and K. H. Bowen, *J. Chem. Phys*., 1998, **108**, 8.
10 R. Weinkauf, J.-P. Schermann and M. S. de Vries, *Eur. Phys. J. D*, 2002, **20**, 309.
11 O. Dolgounitcheva, V. G. Zakrzewski and J. V. Ortiz, *J. Phys. Chem. A*, 1999, **103**, 7912.
12 Smets, D. M. A. Smith, Y. Elkadi and L. Adamowicz, *J. Phys. Chem. A*, 1997, **101**, 9152.
13 N. A. Oyler and L. Adamowicz, *J. Phys. Chem*., 1993, **97**, 11122.
14 M. D. Sevilla, B. Besler and A. O. Colson, *J. Phys. Chem*., 1995, **99**, 1060.
15 S. S. Wesolowski, M. L. Leininger, P. N. Pentchev and H. F. Schaefer III, *J. Am. Chem. Soc*., 2001, **123**, 4023.
16 M. Gutowski *et al*., in preparation.
17 K. Aflatooni, G. A. Gallup and P. D. Burrow, *J. Phys. Chem. A*, 1998, **102**, 6205.
18 P. O. Lowdin, *Rev. Mod. Phys*., 1963, **35**, 724.
19 P. Hobza and J. Sponer, *Chem. Rev*., 1999, **99**, 3247.
20 X. Li, Z. Cai and M. D. Sevilla, *J. Phys. Chem. A*, 2001, **105**, 10115.
21 Y. Podolan, L. Gorb and J. Leszczynski, *Int. J. Mol. Sci*., 2003, **4**, 410.
22 M. Gutowski, I. Dąbkowska, J. Rak, S. Xu, J. M. Nilles, D. Radisic and K. H. Bowen Jr., *Eur. Phys. J. D*, 2002, **20**, 431.
23 I. Dąbkowska, J. Rak, M. Gutowski, J. M. Nilles, S. T. Stokes and K. H. Bowen Jr., *J. Chem. Phys*., 2004, **120**, 6064.
24 M. Haranczyk, I. Dąbkowska, J. Rak, M. Gutowski, J. M. Nilles, S. Stokes, D. Radisic and K. H. Bowen Jr., *J. Phys. Chem. B*, 2004, **108**, 6919.
25 M. Haranczyk, R. Bachorz, J. Rak, M. Gutowski, J. M. Nilles, S. T. Stokes, D. Radisic and K. H. Bowen Jr., *J. Phys. Chem. B*, 2003, **107**, 7889.
26 M. Haranczyk, J. Rak, M. Gutowski, D. Radisic, S. T. Stokes and K. H. Bowen Jr., *Isr. J. Chem*., 2004, **44**, accepted for publication.
27 M. Haranczyk and M. Gutowski, *Internet Electronic Journal of Molecular Design (IEJMD)*, November 23–December 6, 2003, http://www.biochempress.com.
28 I. Dabkowska *et al*., in preparation.
29 J. V. Coe, J. T. Snodgrass, C. B. Freidhoff, K. M. McHugh and K. H. Bowen, *J. Chem. Phys*., 1987, **87**, 4302.
30 J. V. Coe, J. T. Snodgrass, C. B. Freidhoff, K. M. McHugh and K. H. Bowen, *J. Chem. Phys*., 1986, **84**, 618.
31 I. Dąbkowska, J. Rak and M. Gutowski, *J. Phys. Chem. A*, 2002, **106**, 7423.
32 P. Hohenberg and W. Kohn, *Phys. Rev*., 1964, **136**, B864–B871.
33 W. Kohn and L. J. Sham, *Phys. Rev*., 1965, **140**, A1133–A1138.
34 A. D. Becke, *Phys. Rev. A*, 1988, **38**, 3098.
35 A. D. Becke, *J. Chem. Phys*., 1993, **98**, 5648.
36 C. Lee, W. Yang and R. G. Paar, *Phys. Rev. B*, 1988, **37**, 785.
37 B. J. Lynch, P. L. Fast, M. Harris and D. G. Truhlar, *J. Phys. Chem. A*, 2000, **104**, 21.
38 M. J. Frisch, *et al*., Gaussian, Inc., Pittsburgh PA, 1998.
39 T. van Mourik, S. L. Price and D. C. Clary, *J. Phys. Chem. A*, 1999, **103**, 1611.
40 J. C. Rienstra-Kiracofe, G. S. Tschumper and H. F. Schaefer III, *Chem. Rev*., 2002, **102**, 231.
41 R. J. Harrison, *et al*., *NWChem, A Computational Chemistry Package for Parallel Computers Version 4.0.1 2001*, Pacific Northwest National Laboratory, Richland, Washington 99352-0999, USA.
42 M. Gutowski, P. Skurski and J. Simons, *J. Am. Chem. Soc*., 2000, **122**, 10159.
43 K. Aflatooni, B. Hitt, G. A. Gallup and P. D. Burrow, *J. Chem. Phys*., 2001, **115**, 6489.
44 P. Skurski and J. Simons, *J. Chem. Phys*., 2000, **112**, 6568.
45 A. F. Jalbout, K. Y. Pichugin and L. Adamowicz, *Europ. Phys. J. D*, 2003, **26**(2), 197.